Remote monitoring system for detection of faults in drive motors of electric vehicles

Amiya Ranjan Mohanty[1], Nagesh Dewangan[2]

[1,2]*Department of Mechanical Engineering, Indian Institute of Technology Kharagpur, Kharagpur, West Bengal, 721302, India*

amohanty@mech.iitkgp.ac.in
nagesh@iitkgp.ac.in

ABSTRACT

Electric vehicles (EVs) rely on electric motors (EMs) for drive, offering an eco-friendly alternative to conventional internal combustion engines. However, EMs in EVs are prone to multiple defects, such as bearing faults and load torque fluctuations, induced by electromagnetic interference (EMI), mechanical misalignments, and variable loading conditions arising from dynamic driving environments and controller-induced torque ripple. The resulting external mechanical load on the electric motor, which in turn modulates the stator current, produces distinct fault-related frequency components in the motor stator current spectrum. This study presents a system for remotely monitoring the health of such EMs which are used to drive EVs. A non-invasive fault detection methodology using Motor Current Signature Analysis (MCSA) which has come of age in present day to detect and characterize bearing-related faults and load torque fluctuations is used. The proposed approach is examined and validated on permanent magnet synchronous motors (PMSM), which are predominantly used as drive motors in EVs. A hall effect current sensor in one situation and a current transformer (CT) in another have been used to measure the current waveform of the stator current in the PMSM motors, which is then analyzed using the principles of MCSA. MCSA identifies the fault frequencies associated with bearing defects and torque fluctuations without requiring motor disassembly or additional vibration sensors. By implementing MCSA into a standalone monitoring system, this study demonstrates a reliable means of detecting bearing and load torque-related faults, ultimately improving the durability, efficiency, and operational safety of electric vehicle drivetrains. Future work can explore scaling this approach with cyber-physical system (CPS)-based architectures for real-time monitoring of EVs, enabling centralized analytics and smart decision-making as has been showcased in the present work.

1. INTRODUCTION

Electric vehicles (EVs) primarily use electric motors (EMs) as a prime mover for their drivetrain (Thangavel, Deepak, Girijaprasanna, Raju, Dhanamjayulu, & Muyeen, 2023). The power source for these EMs is a battery. Due to limits on emissions and a low carbon footprint in the ecosystem, worldwide, everyone is moving away from traditional internal combustion engines for powering vehicles and looking for EMs in vehicles powered by non-hydrocarbon-based fuel sources, ranging from pure hydrogen to solar to lithium-ion, sodium-ion based batteries (Kachhwaha, Shah, & Shimin, 2016). Active research is being pursued as an alternate energy source for these EMs in electric vehicles.

Many different types of EMs are being used in electric vehicles nowadays, which depend on the power consumption, peak power requirement, speed, control, cost, etc. To name a few, some of these motors are permanent magnet synchronous motors (PMSMs) and induction motors (IMs), brushless direct current (BLDC) motors, etc. (Yildirim, Polat, & Kürüm, 2014). EVs are susceptible to a specific vulnerability when utilizing motor controllers tailored to their unique propulsion needs (Pal & Mohanty, 2020). These controllers, essential for managing speed and torque, introduce electromagnetic interference (EMI) within the electric motors (EMs). EMI can induce bearing faults by generating electrical currents along the motor's shaft, infiltrating the bearings (Rai & Mohanty, 2007; Prabhakar, Mohanty & Sekhar, 2002). These currents, known as bearing or shaft currents, initiate a damaging cycle within the bearing structure, leading to gradual issues like pitting and fluting, compromising bearing integrity. Over time, these detrimental currents can result in significant problems within the motor's bearings and pose a risk to the adjacent gearbox, potentially causing catastrophic failure (Kar & Mohanty, 2006).

To proactively address these vulnerabilities and ensure uninterrupted EM performance in EVs, non-invasive fault detection methodologies are indispensable. Motor current signature analysis (MCSA) proves particularly valuable to detect faults in EMs (Thomson & Fenger, 2001). MCSA has been used to detect faults in rotor bars, stator winding, air-gap eccentricity, bearing, and load torque fluctuations of a motor (Cameron, Thomson & Dow, 1986; Thomson, Chalmers & Rankin, 1987; Thomson & Chalmers, 1988; Thomson, 2001; Blodt, Regnier & Faucher, 2009). MCSA permits real-time assessments of motor health during active operation, enabling EV owners and manufacturers to pinpoint and detect issues without necessitating motor disassembly or operational downtime. This approach significantly enhances EV reliability and durability, reducing maintenance costs and bolstering customer satisfaction (Lei, Yang, Jiang, Jia, Li & Nandi, 2020).

Furthermore, various machine learning (ML) models have been employed to diagnose faults in motors using current and vibration signals. Centrifugal pumps have been investigated for fault diagnosis using a multi-class Support Vector Machine (SVM) with optimized hyperparameters to classify five categories: Healthy, Vane tip fault, Cracked impeller, Leakage, and Cavitation (Araste, Sadighi, & Moghaddam, 2020). They achieved high classification accuracy for both healthy and leakage conditions, as well as above-average accuracy for cavitation. Similarly, Stator winding faults have been detected and classified based on the amplitudes of harmonics, mean, and root mean square (RMS) values of the current spectrum, as well as SVM (Pietrzak & Wolkiewicz, 2021). They identified multiple severity levels using this approach and achieved an accuracy of 97% on test data. Later, a two-class autoencoder model has been examined for fault detection in centrifugal pumps using vibration signals (Vasiliev, Frangu, & Cristea, 2022). They investigated autoencoder models in both feed-forward and convolutional settings to extract sensitive features to detect faults by training models based on normal operating conditions.

This article outlines a fault detection methodology for various faults, integrating real-time remote monitoring of the motor's health during its operation. Bearing and load torque fluctuations typically yield distinct fault frequency signatures within the vibration spectrum, resulting in fluctuations in electromagnetic torque. Consequently, fault frequencies manifest as additional spectral components around the supply line frequency in the motor current spectrum. These detection techniques seamlessly integrate into a broader cyber-physical system (CPS), merging digital technologies with physical machinery to enhance overall system reliability and performance. The article illustrates the on-field implementation of MCSA-based fault detection within a CPS-based architecture, executed automatically without human intervention. Furthermore, the article examines fault detection using an ML model based on current signals. Detecting faults in PMSM motors is crucial to enhancing overall system reliability.

2. FAULT DETECTION IN PMSM

2.1. Bearing Fault Detection Using MCSA

The PMSM is a specialized three-phase synchronous motor featuring rare-earth permanent magnets, offering advantages such as compactness, high power-to-weight ratio, precise torque control, and efficiency. However, PMSMs are susceptible to electrical, magnetic, or mechanical faults during prolonged operation in challenging conditions, posing risks to machine reliability and its safety. To address these issues, early detection through real-time monitoring is vital. Bearing faults are particularly common contributors to motor failures, impacting the system's vibration and motor current signatures as they progress. Here focus is given to investigate bearing faults in PMSMs, considering fault severity and motor speed effects. Bearing defects generate impulses during each shaft rotation (Pal & Mohanty, 2022), leading to torque pulsations and a characteristic fault frequency (CFF) denoted as f_{BPFO} in Eq. (1).

$$f_{BPFO} = N_b \frac{f_m}{2}\left(1 - \frac{BD}{PD}\cos\beta\right) \quad (1)$$

where, f_m is the motor rotational frequency, N_b is number of balls in the bearing; and BD, PD and β represent ball diameter, pitch diameter, and contact angle of the bearing, respectively.

The bearing vibrations affect the motor current. Bearing defects disrupt magnetic flux, altering electromagnetic torque, and causing amplitude modulation with CFFs around f_s. For outer race defects, these CFFs appear as sidebands expressed in Eq. (2).

$$f_{Bearing} = f_s \pm k f_{BPFO} \quad (2)$$

where, k is an integer 1, 2, 3…

2.2. Load Torque Fluctuation Detection Using MCSA

Load torque fluctuation refers to the periodic variation in the mechanical torque load applied to an electric motor, typically due to uneven or cyclic mechanical loads such as imbalance, misalignment, or other mechanical interactions. When a motor operates under a fluctuating load torque, the mechanical variations at the frequency interact with the electromagnetic field of the motor. This interaction modulates the stator current and air-gap flux density, leading to the generation of sideband frequencies around the fundamental supply frequency. The torque fluctuation acts as a low-frequency modulating signal, while the stator current fundamental frequency serves as the carrier signal. Torque fluctuations disrupt the magnetic flux, altering electromagnetic torque, and generate sidebands around the supply frequency as f_s in Eq. (3).

$$f_l = f_s \pm f_L \quad (3)$$

where, f_L is the load torque fluctuation frequency, f_l is the sideband frequency, respectively.

2.3. Unsupervised autoencoder model

To perform unsupervised anomaly detection on multivariate sensor data, a fully connected autoencoder architecture has been developed. The autoencoder receives an n-dimensional feature vector as input and learns a compressed latent representation through a bottleneck structure. The network consists of two main components: an encoder and a decoder. The encoder progressively reduces dimensionality using a series of linear transformations with nonlinear activation functions (e.g., ReLU). The decoder mirrors the encoder, reconstructing the original feature space from the latent vector. During training, the network minimizes the error between the input and the reconstructed output, enabling the autoencoder to model the normal operating condition of the system. These errors are compared against a threshold to determine whether the input data corresponds to a normal or abnormal condition. Overall, the autoencoder is effective for fault detection because it does not require labeled fault data.

3. METHODOLOGY OF FAULT DETECTION

The present study explores motor current analysis, focusing on detecting faults by measuring the motor current waveform in one of the phases. Two different motors with different defects have been examined: one motor with outer race defects in bearings and another with load torque fluctuations. The complete experimental setup of both motors is provided in Sections 3.1 and 3.2. Later, an autoencoder model is used to detect these defects in the motor as an anomaly.

3.1. Experimental Setup for Bearing Defect Detection

In this study, a 1 kW PMSM was tested as shown in Figure 1 with motor parameters as depicted in Table 1. A PWM adjustable speed drive controlled it while subjected to load via a DC generator and a resistor bank. Data from the phase stator winding's current were collected using a Hall effect current probe (Tektronix A622) and a National Instruments data acquisition system (NI-DAQ 9215) with a sampling frequency of 10 kHz. The primary focus was on the drive end bearing, with Table 2 showing bearing dimensions. Three sets of bearings were used: one healthy (Brg-1), and two artificially faulted (Brg-2 and Brg-3) using electro-discharge machining, with Brg-3 exhibiting more significant faults than Brg-2 as depicted in Table 3.

Table 1. PMSM M0 parameters.

Parameter	Value
Rated power	1 kW
Rated speed	3000 RPM
Rated voltage	48 V
Rated current	21 A
Number of pole pairs	5
No. of phases	3
Bearing number	6206

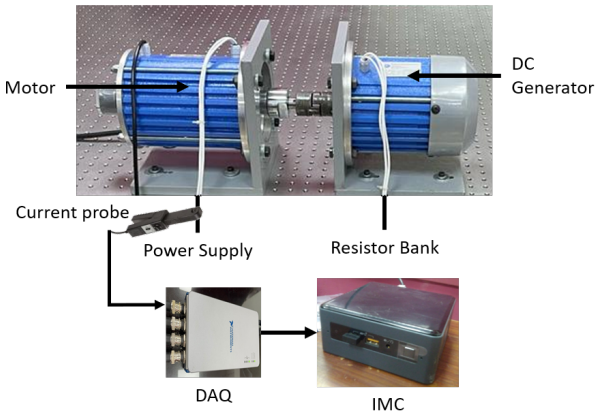

Figure 1. Laboratory-level experimental setup for EV.

Table 2. Specifications of bearing 6206.

Parameter	Value
Ball diameter	10 mm
Pitch diameter	46 mm
Contact angle	0º
Number of balls	9
Ball diameter	10 mm

Table 3. Specifications of defect in bearings of PMSM.

Bearing type	Fault dimensions (width X breath X thickness)
Healthy bearing (Brg-1)	-
Faulty bearing 1 (Brg-2)	1 mm X 1 mm X 0.1 mm
Faulty bearing 2 (Brg-3)	2 mm X 2 mm X 0.1 mm

3.2. Experimental Setup for Load Torque Fluctuation

In this study, a 1 kW PMSM was tested as shown in Figure 2 with motor parameters as depicted in Table 4. Data from a phase stator winding's current was collected with a YMDC SCT013 split core current transformer (CT) and the data acquisition system with a sampling frequency of 10 kHz, as detailed in Section 3.1. The primary focus was on the load torque fluctuation due to defective cooling fan blades. To simulate different mechanical unbalance load conditions on motor, three sets of fan blades were used, as depicted in Figure 3 and provided in Table 5.

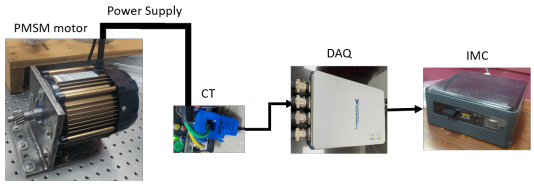

Figure 2. Experimental setup for load torque fluctuation.

Table 4. PMSM M1 parameters.

Parameter	Value
Rated power	1 kW
Rated speed	3000 RPM
Rated voltage	48 V
Rated current	21 A
Maximum current	50 A
Rated power	1000 W
Peak power	2139 W
Rated speed	3000 RPM
Max speed	3500 RPM
No. of pole pairs	5
No. of phases	3
Bearing number	6203

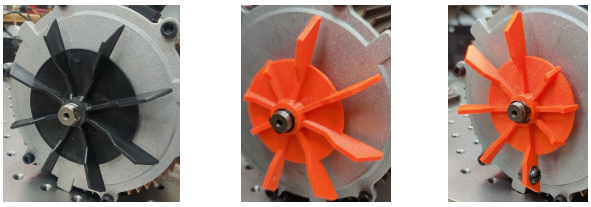

(a) (b) (c)

Figure 3. View of the seeded defects on cooling fan of PMSM: Normal (b) 3 blades removed (c) 3 blades removed+ nut and bolt.

Table 5. Specifications of torque fluctuation defect.

Fan blade condition	Load condition
Healthy fan (Fb-1)	Normal fan blades
Faulty fan 1 (Fb-2)	3 blades removed
Faulty fab 2 (Fb-3)	3 blades removed + nut and bolt

3.3. Autoencoder for fault detection

An autoencoder model is developed for fault detection using eight input features: spectral Energy, Spectral Centroid, Spectral spread, spectral entropy, mean frequency, standard deviation of frequency, spectral kurtosis, and spectral skewness. The encoder sequentially reduces the feature space through layers (8, 256, 128, 64, 32) using ReLU activations to capture nonlinear relationships. The decoder mirrors this structure (32, 64, 128, 256, 8), reconstructing the original input. By minimizing reconstruction error, the model learns normal data behavior and identifies anomalies when reconstruction deviation is high. The Adam optimizer with a learning rate of 0.001 and a weight decay of 10^{-4} has been implemented. The trained model predicted two classes: either normal or abnormal, based on the test data.

4. REMOTE FAULT DETECTION OF EVS USING MCSA

A demonstration of remote monitoring using MCSA is showcased to detect two different fault types: bearing faults and load torque fluctuations. An industrial mini-computer (IMC) processes data wirelessly acquired from a data acquisition (DAQ) system operating at a sampling frequency of 10 kHz, identifying fault occurrences with a binary value of 0 or 1. These binary values, alongside corresponding current spectrum data, were saved in separate CSV files, which were then uploaded to Google Cloud Storage (GCS) for the electric vehicle workshop personnel to access the motor condition. This framework forms a CPS that provides sustainable and remote motor health monitoring.

4.1. Architecture of Remote Fault Detection

The proposed CPS enables real-time motor health assessment with minimal human intervention, thereby enhancing overall operational reliability. It integrates electromagnetic modules, current sensors, wireless data acquisition, an IMC, and GCS, as illustrated in Figure 4. The IMC performed Fast Fourier Transform (FFT) analysis on the acquired current signals to extract CFFs that indicate potential motor abnormalities. The processed results and detection reports were compiled into CSV files and automatically uploaded to GCS for centralized access and remote decision-making. This approach ensures timely fault detection, maintenance scheduling, and rapid issue resolution, ultimately improving electric vehicle reliability and availability. This system can also provide updates to the vehicle driver in the dashboard display or a mobile application.

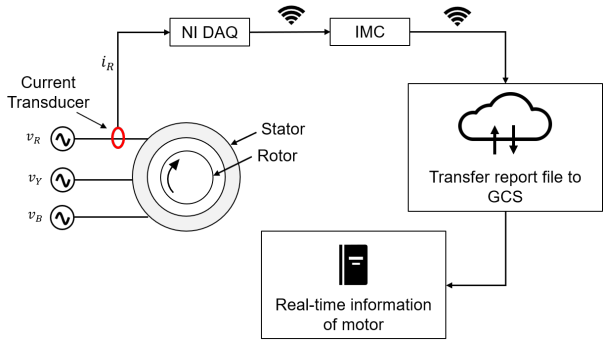

Figure 4. Architecture of remote fault detection.

4.2. Experimental Setup for Remote Fault Detection

In an experiment utilizing a CPS for motor health and fault detection, two motors (M0, M1) with specifications provided

in Tables 1 and 4 were employed, and the setup is illustrated in Figure 5. An Intel NUC served as the central processing unit, while a current probe measured the stator winding current for motor M0, and a CT measured the stator winding current for motor M1. Data was collected using a National Instruments (NI) 4-channel voltage input module (NI-9215), wirelessly connected to an IMC via a DAQ chassis (NI-9191). An autonomous IMC software application detected CFFs without human intervention and employed the Google Cloud SDK for connectivity to GCS. Reports were stored as CSV files and securely uploaded to a dedicated GCS storage bucket via HTTP with TLS encryption, with GCS preserving metadata for tracking fault timing. Communication utilized the 802.11 internet protocol between the DAQ, IMC, and GCS.

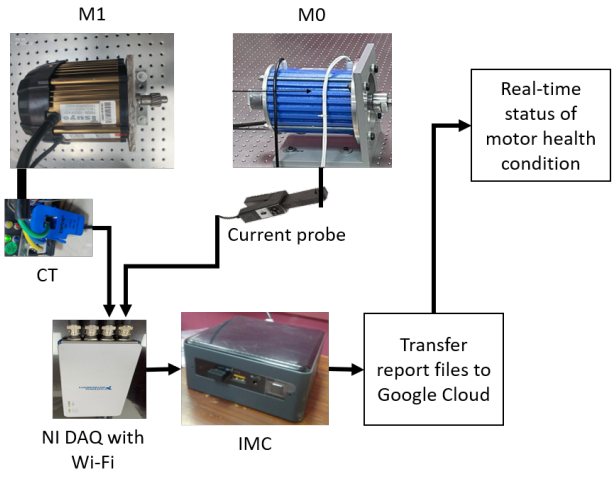

Figure 5. EMs real-time fault detection experiment setup.

5. RESULTS

5.1. Bearing Fault Detection in PMSM

The PMSM motor M0 was run at 2220 RPM, with the current's time-domain waveform shown in Figure 6(a). FFT with a logarithmic scale was applied to analyze the signal, and a Hanning window prevented spectral leakage. Using bearing dimensions from Table 2 in Eq. (1), the f_{BPFO} value was calculated as 130.30 Hz at 2220 RPM. Vibration-induced torque pulsations affected electromagnetic torque, causing harmonics to appear in current spectrum as sidebands at the frequency of $(f_s + f_{BPFO})$. At 2220 RPM, $(f_s + f_{BPFO})$ was determined as 315.30 Hz (Figure 6(b)). An increase in fault severity at given motor speed led to higher current amplitudes corresponding to $(f_s + f_{BPFO})$, as detailed in Table 6. For motor M0, operating at a 50 Hz supply frequency, a bearing fault (Brg-2) was introduced. The corresponding CFFs were successfully identified, and the fault was detected, as indicated by a Boolean value of "1", as shown in Figure 7.

Table 6. Current amplitude {Log (Current [A])} corresponding to bearing faults.

Bearing type	Current amplitude (dB)
Brg-1	-50.12 dB
Brg-2	-45.17 dB
Brg-3	-41.65 dB

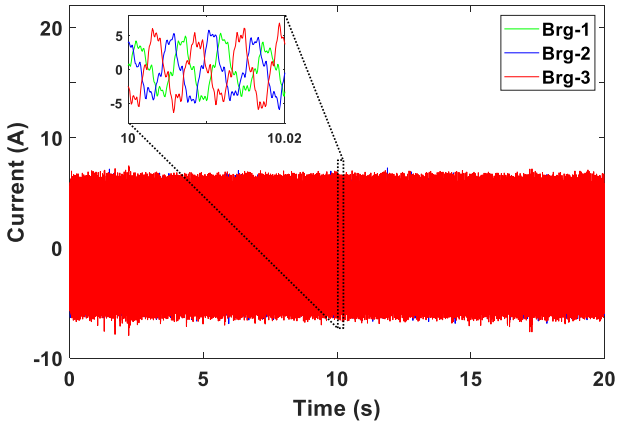

(a)

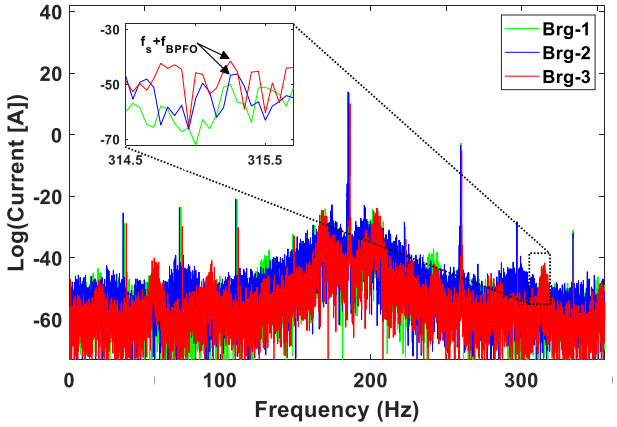

(b)

Figure 6. (a) Current time-domain signal, (b) Current spectrum, of healthy and faulty bearings for f_m=37 Hz.

	A	B	C	D
1	Developed at Indian Institute of Technology Kharagpur			
2				
3	Rotor fault	0		
4	Stator winding fault	0		
5	Eccentricity fault	0		
6	Bearing fault	1		
7	Torque fluctuations	0		
8				

Figure 7. Boolean report for bearing fault in motor M0.

5.2. Detection of Load Torque Fluctuation

Similarly, the process involves recording the time-domain current signals from motor M1 at different load conditions (as shown in Figure 3) and converting them into the frequency domain using FFT. The motor M1 was run at 3450 RPM with the current's time domain waveform, as shown in Figure 8(a). At 3450 RPM, the supply frequency was calculated to be 287.5 Hz, as shown in Figure 8(b). The software then analyzes the spectrum to identify CFFs caused by load torque fluctuations. When fault severity increases from normal to the removal of fan blades and unbalance mass, current amplitudes increase, as detailed in Table 7. These fluctuations appear as sidebands around the main supply frequency at $(f_s \pm f_L)$ with a Boolean value of "1" in the report file, which shows "Torque fluctuation" defect. These reports are uploaded to GCS and can be remotely accessed by plant personnel to monitor motor performance, detect torque-related issues early, and take corrective actions to maintain smooth and reliable operation.

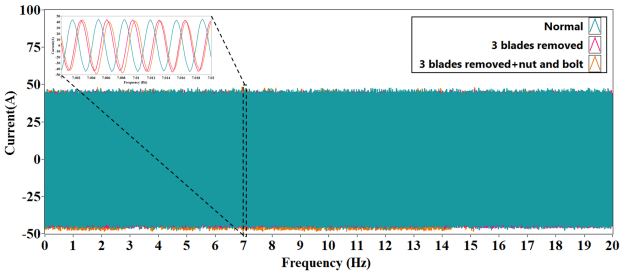

(a)

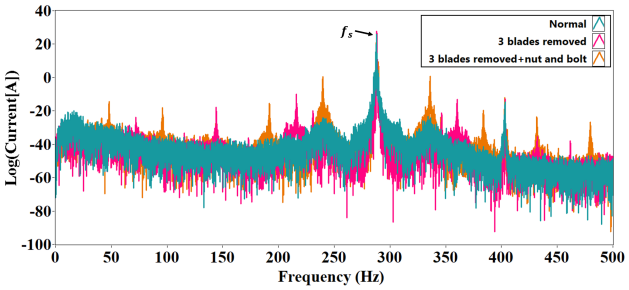

(b)

Figure 8. (a) Current time-domain signal, (b) Current spectrum of load torque fluctuation.

Table 7. Current amplitude {Log (Current [A])} corresponding to torque fluctuation.

Load condition	Current amplitude (dB)
Fb-1	-24.28 dB
Fb-2	-12.98 dB
Fb-3	1.01 dB

5.3. Fault detection as anomaly using autoencoder model

The current data from the PMSM motor, as mentioned in Section 3.2, has been utilized for fault detection using an autoencoder model. A total of 240 datasets were created to test the model, with 80 datasets for each kind of fault. The autoencoder model was trained on a dataset of normal conditions and tested on both normal and faulty conditions. The test results are presented in Table 8. The autoencoder model predicted zero anomaly for the normal condition of the fan blade, whereas 98.75% and 91.25% of anomaly for the faulty conditions. This showed that one input of the Fb-2 load condition (3 blades removed) and seven inputs of Fb-3 load condition (3 blades removed + nut and bolt) cases were misclassified as the normal condition. This clarified that additional features are needed to improve the prediction accuracy of the Fb-3 load condition, specifically in terms of frequency content.

Table 8. Anomaly prediction for load conditions.

Load condition	Test data	Predicted	Accuracy (%)
Fb-1	80	80 (Normal)	100
Fb-2	80	79 (Anomaly)	98.75
Fb-3	80	73 (Anomaly)	91.25

6. CONCLUSIONS

Permanent magnet synchronous motors (PMSMs) in electric vehicles offer high efficiency and power density, ensuring precise control for optimized performance. However, motor controllers for EVs can introduce electromagnetic interference (EMI), leading to bearing faults due to induced shaft currents and other faults related to load torque fluctuations. Non-invasive detection methods, such as motor current signature analysis (MCSA), are crucial for ensuring the reliability of EM. The MCSA was implemented on a remote monitoring system through a cyber-physical system (CPS) to enable detectability from a remote location. The proposed monitoring approach successfully detected bearing and load torque fluctuation faults in two PMSM motors remotely. Further, the implemented autoencoder model was able to predict faults as anomalies in the PMSM motor. This monitoring solution can be integrated with CPS-based architectures for real-time monitoring, better automation, smart maintenance planning, and decision-making in electric motor health management for EVs.

ACKNOWLEDGEMENT

Authors would like to express their gratitude to Dr. Pal Ranjan Sasti Charan, a PhD graduate from the Department of Mechanical Engineering, Indian Institute of Technology Kharagpur, for his support in collecting the data.

REFERENCES

Araste, Z., Sadighi, A., & Moghaddam, M.J. (2020). Support Vector Machine-Based Fault Diagnosis of a Centrifugal Pump Using Electrical Signature Analysis. *Proceedings of the 6th Iran. Conf. Signal Process. Intell. Syst. ICSPIS 2020*. https://doi.org/10.1109/ICSPIS51611.2020.9349554

Blodt, M., Regnier, J., & Faucher, J. (2009). Distinguishing load torque oscillations and eccentricity faults in induction motors using stator current Wigner distributions. *IEEE Transactions on Industry Applications*, vol. 45, No. 6, pp. 1991–2000. doi: 10.1109/TIA.2009.2039973

Cameron, J. R., Thomson, W. T., & Dow, A. B. (1986). Vibration and current monitoring for detecting airgap eccentricity in large induction motors. In *Proceedings of the Institution of Electrical Engineers*, 133(B), pp. 155–163. doi: 10.1049/ip-b.1986.0022

Kar, C., & Mohanty, A. R. (2006). Monitoring gear vibrations through motor current signature analysis and wavelet transform. *Mechanical Systems and Signal Processing*, vol. 20, No. 1, pp. 158–187. doi: 10.1016/j.ymssp.2004.07.006

Kar, C., & Mohanty, A. R. (2006). Multistage gearbox condition monitoring using motor current signature analysis and Kolmogorov–Smirnov test. *Journal of Sound and Vibration,* vol. 290 (1–2), pp. 337–368. doi: 10.1016/j.jsv.2005.04.020

Kachhwaha, A., Shah, V. A., & Shimin, V. V. (2016, November). Integration methodology of ultracapacitor-battery based hybrid energy storage system for electrical vehicle power management. *Proceedings of the 2016 IEEE 7th Power India International Conference (PIICON)* (p. 1–6). IEEE. doi: 10.1109/POWERI.2016.8077231

Lei, Y., Yang, B., Jiang, X., Jia, F., Li, N., & Nandi, A. K. (2020). Applications of machine learning to machine fault diagnosis: A review and roadmap. *Mechanical Systems and Signal Processing,* vol. 138, No. 106587. doi: 10.1016/j.ymssp.2019.106587

Mohanty, A. R., & Pal, R. S. C. (2021). A cyber-physical system based real-time fault diagnosis of induction motors. In *Structural Health Monitoring 2021 Conference* (p. 1–10). doi: 10.12783/shm2021/36275

Nkwinika, R. & Muteba, M. (2025). Detection of Broken Rotor Bars in Induction Motors Using Supervised Machine Learning Methods. In *Proceedings of 33rd South. African Univ. Power Eng. Conf. SAUPEC 2025* (p. 1–5). https://doi.org/10.1109/SAUPEC65723.2025.10944335

Pal, R. S. C., & Mohanty, A. R. (2020). A simplified dynamical model of mixed eccentricity fault in a three-phase induction motor. *IEEE Transactions on Industrial Electronics, 68*(5), (p. 4341–4350). doi: 10.1109/TIE.2020.2987274

Pal, R. S. C., & Mohanty, A. R. (2022). Bearing fault detection in permanent magnet synchronous motors using vibration and motor current signature analysis. *Proceedings of the 28th International Congress on Sound and Vibration* (p. 1–6), July 24–28, Singapore.

Pietrzak, P., & Wolkiewicz, M. (2021). Application of Support Vector Machine to stator winding fault detection and classification of permanent magnet synchronous motor. *Proceedings of 2021 IEEE 19th Int. Power Electron. Motion Control Conf. PEMC 2021* (p. 880–887). https://doi.org/10.1109/PEMC48073.2021.9432629

Prabhakar, S., Mohanty, A. R., & Sekhar, A. S. (2002). Application of discrete wavelet transform for detection of ball bearing race faults. *Tribology International,* vol. 35, No. 12, pp. 793–800. doi: 10.1016/S0301-679X(02)00063-4

Rai, V. K., & Mohanty, A. R. (2007). Bearing fault diagnosis using FFT of intrinsic mode functions in Hilbert–Huang transform. *Mechanical Systems and Signal Processing,* vol. 21, No. 6, pp. 2607–2615. doi: 10.1016/j.ymssp.2006.12.004

Thangavel, S., Deepak, M., Girijaprasanna, T., Raju, S., Dhanamjayulu, C., & Muyeen, S. M. (2023). A comprehensive review on electric vehicle: battery management system, charging station, traction motors. *IEEE Access*. doi: 10.1109/ACCESS.2023.3250221

Thomson, W. T., & Fenger, M. (2001). Current signature analysis to detect induction motor faults. *IEEE Industry Applications Magazine*, 7(4), 26–34. doi: 10.1109/2943.930988

Thomson, W. T., Chalmers, S. J., & Rankin, D. (1987, September). On-line current monitoring fault diagnosis in HV induction motors – case histories and cost savings in offshore installations. Paper presented at *SPE Offshore Europe*, Aberdeen, United Kingdom. doi: 10.2118/16577-MS

Thomson, W. T., & Chalmers, S. J. (1988). A new on-line computer based current monitoring system for expert system fault diagnosis of induction motors. *Proceedings of the UPEC'88 (p. 104–109)*. Trent Polytechnic, Nottingham, England.

Thomson, W. T. (2001). On-line MCSA to diagnose shorted turns in low voltage stator windings of 3-phase induction motors prior to failure. *Proceedings of the IEEE International Electric Machines and Drives Conference (IEMDC 2001)* (Cat. No.01EX485) (p. 891–898). Cambridge, MA, USA. doi: 10.1109/IEMDC.2001.939425

Vasiliev, I., Frangu, L., & Cristea, M.L. (2022). Pump Fault Detection Using Autoencoding Neural Network. Proceedings of the 26th Int. Conf. Syst. Theory, Control Comput. 426–431. https://doi.org/10.1109/ICSTCC55426.2022.9931848

Yildirim, M., Polat, M., & Kürüm, H. (2014, September). A survey on comparison of electric motor types and drives

used for electric vehicles. *Proceedings of the 2014 16th International Power Electronics and Motion Control Conference and Exposition* (p. 218–223). IEEE. doi: 10.1109/EPEPEMC.2014.6980715

BIOGRAPHIES

Amiya Ranjan Mohanty received the B.Sc. Engg. (Hons.) degree in Mechanical Engineering from the National Institute of Technology, Rourkela, India, in 1986, and M.Tech. degree in the area of Machine Design from the Indian Institute of Technology, Kharagpur, India, in 1988. He received his Ph.D. degree in the area of Noise Control from the University of Kentucky, Lexington, USA, in 1993. He was associated with the Ray W. Herrick Laboratories, School of Mechanical Engineering, Purdue University, West Lafayette, USA, as a Postdoctoral Fellow, working in the areas of active noise control. Presently, he is the BIS Standardization Chair Professor in the Department of Mechanical Engineering at IIT Kharagpur, India. His research interests are in the areas of cyber-physical systems, internet of things, machinery condition monitoring, fault diagnosis and prognosis, underwater acoustics, signal processing, machine learning, acoustics, and noise control. He has worked in the R&D Division of Larsen and Toubro Ltd., Mumbai, India, in the area of machinery condition monitoring. He has also worked in Ford Motor Company, Detroit, MI, in the area of automobile Computer Aided Engineering/Noise Vibration & Harshness (CAE/NVH).

Nagesh Dewangan received the B.E. degree in Mechanical Engineering from the Bhilai Institute of Technology, Durg, India, in 2016, and M.Tech. degree in Maintenance Engineering & Tribology from the Indian Institute of Technology (ISM), Dhanbad, India, in 2019. He is currently a Doctoral Researcher in the Acoustics and Condition Monitoring Laboratory, Mechanical Engineering Department, Indian Institute of Technology Kharagpur, India. His research interests are in the areas of cyber-physical systems, Internet of Things, machinery condition monitoring, machine learning, signal processing, and product design.